Multifaceted Functionalities of Bridge-Type DC Reactor Fault Current Limiters An Experimentally Validated Investigation

Behdani, Behzad ; Moghim, Ali; Mousavi, Sheyda ; Soltanfar, Mostafa ; Hojabri, Mojgan

DOI
10.3390/en17040975

Publication date
2024

Document Version
Final published version

Published in
Energies

energies

MDPI

Article

Multifaceted Functionalities of Bridge-Type DC Reactor Fault Current Limiters: An Experimentally Validated Investigation

Behzad Behdani [1,*], Ali Moghim [2], Sheyda Mousavi [3], Mostafa Soltanfar [4] and Mojgan Hojabri [5]

[1] Department of Electrical Sustainable Energy, Faculty of Electrical Engineering, Mathematics and Computer Science, Delft University of Technology, 2628 CD Delft, The Netherlands
[2] Department of Electrical Engineering, Zanjan Branch, Islamic Azad University, Zanjan 45156-58145, Iran; ali.moghim@iau.ac.ir
[3] Department of Electrical Engineering, Zanjan University, Zanjan 45371-38791, Iran; sheydamousavi2@gmail.com
[4] Department of Electrical Engineering, University of Kashan, Kashan 87317-53153, Iran; mostafa.soltanfar@gmail.com
[5] Competence Center of Digital Energy and Electric Power, Institute of Electrical Engineering, Lucerne University of Applied Sciences and Arts, 6048 Horw, Switzerland; mojgan.hojabri@hslu.ch
* Correspondence: b.behdani-1@tudelft.nl

Abstract: With the ongoing expansion and interconnection of electrical power systems, alongside the rapid proliferation of renewable distributed generations (DGs), the short-circuit extent in the power grid is experiencing a significant rise. Fault current limiters (FCLs) have been introduced in an effort to address this issue, ensuring the robustness and sustainability of expensive power system components when confronted with short-circuit faults. Among the various types of FCLs, bridge-type DC reactor fault current limiters (BDCR-FCLs) have emerged as one of the most promising options. While BDCR-FCLs have shown excellent properties in limiting harmful short-circuit currents, they are also advantageous in other respects. This paper investigates the supplementary functionalities of BDCR-FCLs as a multifaceted device towards the enhancement of the quality of supplied energy in terms of total harmonic distortion (THD) reduction, power factor (PF) correction, peak current reduction for nonlinear loads, and soft load variation effects, as well as their capability to limit fault current. To this aim, the capabilities of BDCR-FCLs have been studied through various simulated case studies in PSCAD/EMTDC software V5.0.1, in addition to experimental tests considering an AC microgrid connected to a DC system. The experimental and simulation investigations verify the superior multifaceted functionalities BDCR-FCLs introduce in addition to their excellent fault current-limiting capabilities. The results show that PF improved by 6.7% and 7%, respectively, in simulation and experimental tests. Furthermore, the current THD decreased by 20% and 18% in the simulation and experiment, respectively.

Keywords: AC/DC microgrid; bridge-type DC reactor; fault current limiter

Citation: Behdani, B.; Moghim, A.; Mousavi, S.; Soltanfar, M.; Hojabri, M. Multifaceted Functionalities of Bridge-Type DC Reactor Fault Current Limiters: An Experimentally Validated Investigation. *Energies* **2024**, *17*, 975. https://doi.org/10.3390/en17040975

Received: 11 January 2024
Revised: 9 February 2024
Accepted: 16 February 2024
Published: 19 February 2024

1. Introduction

Electrical power systems are undergoing a fundamental transition through the integration of modern power electronic-based equipment and resources while expanding and interconnecting to meet the ever-growing electrical energy demands. This, on the one hand, has increased the complexity and uncertainty of the system and, on the other hand, resulted in the elevation of the short-circuit levels above the tolerable fault current of the installed equipment [1,2]. Consequently, the power system components have become susceptible to failure, leading to significant costs and an increased risk of grid-wide failures. In order to ensure the continued reliability and safe operation of the power system, in terms of the robustness of components against short-circuit faults, the employment of fault current limiters (FCLs) is one of the most effective solutions [3,4]. Various types of FCLs have been

proposed over the years, such as the reactor type [5], solid state type [6], superconductor type [7], and hybrid topologies [8]. The focus of this paper is on bridge-type DC reactor FCLs (BDCR-FCLs), which have gained popularity in the past years due to their superior capabilities.

Series BDCRs have been applied in the protection of modern power grids as efficient fault current-limiting devices [9–11]. In principle, a DC reactor-type FCL operates based on its inductor unit's tendency to oppose current change, thus producing fault current-limiting capabilities to the device [10]. DC reactor-type FCLs have been employed in HVDC networks for fault current limitation as well [11]. In another application, the capabilities of the series DC reactor-type configuration as a dual-function device for both fault current limitation and overvoltage suppression [12]. An AC/DC reactor-type FCL was proposed in [13] to limit the rate of rise of fault current. The study carried out in [13] also demonstrated that the bridge-type series DC reactor FCLs do not impose any reactive power on the network.

One of the most critical challenges in modern electrical energy systems is the introduction of harmonic contents in the network arising from nonlinear loads and inverter-based resources. The IEEE standards [14,15] address this issue, focusing on harmonics content restriction in low and medium-voltage networks. On the consumer side, loads such as high-efficiency lights, computers, light dimmers, battery chargers, adjustable speed drives, heat pumps, electric vehicle battery chargers, etc., have caused serious power quality issues, increasing the total harmonic distortion (THD) in the network to concerning levels [16]. Conventionally, to limit the emitted harmonic content of modern power-electronic-based loads, passive filters formed as interconnected circuits of inductors and capacitors are commonly employed [17]. Along with filters, DC-side ripples can also be alleviated by adding a branch with capacitive and/or resistive elements in the terminals of the rectifier bridge [18]. The addition of a series line inductance on the rectifier bridge was shown to be effective for THD reduction of the full bridge rectifier [19].

There are various types of devices aimed at improving power quality factors [20], utilizing passive [21] or active [22] mechanisms. Typically, these devices are designed to address specific power quality issues rather than functioning as multifunctional equipment [23]. In high-voltage grids, passive power factor (PF) correctors and filters play crucial roles and have been extensively discussed [23–25]. A comprehensive review of passive filter structures for grid-connected voltage-source converters and their ability to reduce harmonic content is provided in [20]. Another important aspect of power quality indicators is their PF correction capability. For nonlinear consumers, a common solution for enhancing PF involves the utilization of series AC reactors, which consist of passive elements (L or C) placed in the AC side of the system [3,26].

In this paper, supplementary functionalities of BDCR-FCLs are investigated. In this regard, the effect of series BDCR-FCLs on THD reduction, PF correction, peak current decrement of nonlinear loads, and soft load variation in the network are studied alongside their fault current-limiting capabilities. It should be noted that although this paper tries to lay out the supplementary functionalities of the BDCR-FCLs besides their main role in limiting fault current, its aim is not solely to propose this device for power quality enhancement. The analyses have been carried out on a test system consisting of an AC microgrid connected to a simple DC microgrid through simulations conducted in PSCAD-EMTDC software and experimental verification using a laboratory test circuit. The rest of this paper is organized as follows. Section 2 outlines the various modes of the distribution network operation with BDCR-FCLs. Section 3 provides an analytical study of the test system. Section 4 presents the simulation and prototype experimental test results. Discussion is made in Section 5, and the study is concluded in Section 6.

2. Analysis of BDCR-FCL Configurations in Microgrids

Throughout this paper, a comprehensive analysis of the BDCR-FCL operation is conducted by examining three distinct scenarios:

- Case 1: An AC microgrid connected to a DC line without the implementation of BDCR-FCL.
- Case 2: A linear load connected to an AC microgrid with a BDCR-FCL installed in series.
- Case 3: An AC microgrid connected to a DC line with the integration of BDCR-FCL.

Since the study in this paper is constructed based on a comparative analysis of the results obtained from these three cases to demonstrate the effect of BDCR-FCL, these three cases are introduced and elaborated in this section.

2.1. Case 1: AC Microgrid Connected to a DC Line without BDCR-FCL

In this case, the network topology is considered based on the connection of an AC microgrid to a DC line through an AC/DC voltage converter. The system configuration is depicted in Figure 1, comprising a full bridge rectifier and a shunt capacitor utilized to reduce the DC voltage ripples. Although the inclusion of large capacitances significantly minimizes voltage ripple on the DC side, it results in a reduction of the time constant for the supplied AC current and thus leads to a substantial increase in AC current peak value [27].

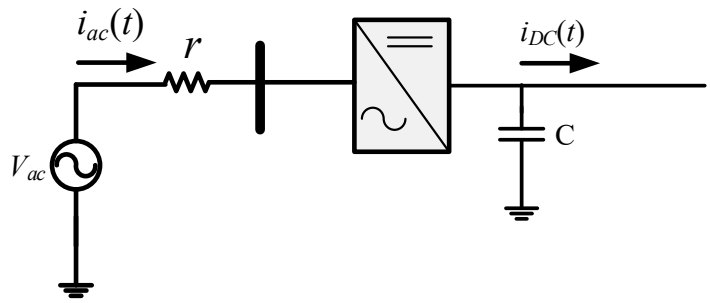

Figure 1. Topology of an AC microgrid to a DC line through a converter, without BDCR-FCL.

2.2. Case 2: BDCR-FCL Connected in Series to an AC Load in an AC Microgrid

As can be seen in Figure 2, a BDCR-FCL can be considered in the form of a DC reactor-type FCL interfaced with a bridge rectifier. In this circuit, the inductance L_d and resistor r_d belong to the DC reactor, while diodes D1 to D4 form the rectifying bridge that converts the AC current of the network to the reactor's DC current i_{DCR}. It is worth noting that the source's current i_{ac} is approximately equal to the load current i_L. In the steady state, the rectifier bridge charges the BDCR-FCL, keeping its current around a particular DC value, and the voltage drop on the BDCR-FCL is negligible. However, in the transient state, the voltage drop of the BDCR-FCL changes accordingly to compensate for any current surge or fault, smoothing the supplied current to the load.

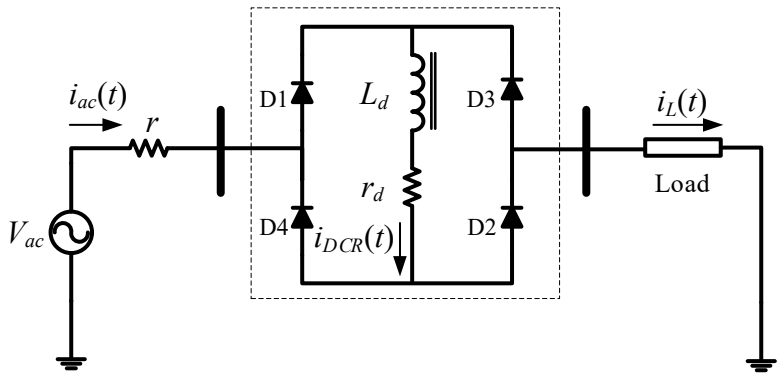

Figure 2. Topology of a series BDCR-FCL connected in an AC microgrid.

2.3. Case 3: BDCR-FCL Incorporated with an AC Microgrid Connected to a DC Line

Figure 3 illustrates a BDCR-FCL interfaced with an AC/DC converter, linking an AC microgrid to a DC line. Besides providing fault current-limiting capabilities, this configuration introduces other functionalities, such as THD reduction, PF correction, and nonlinear load peak current decrement, which will be demonstrated later. These additional advantages are of special interest where design size becomes a constraint, reducing the need for bulky extra power quality enhancement filters.

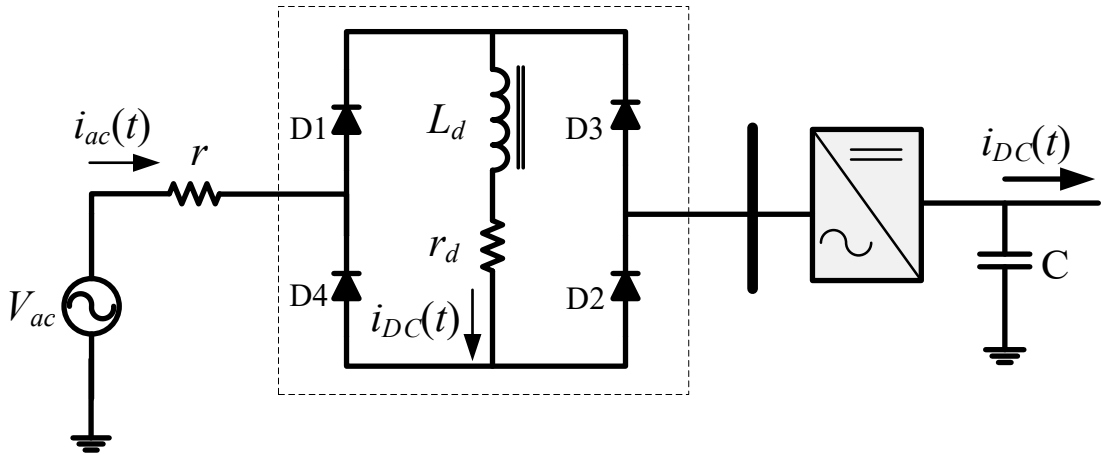

Figure 3. Topology of a series BDCR-FCL incorporated with an AC microgrid connected to a DC line.

In Figure 4, an example network has been shown where an AC microgrid consisting of renewable and fuel-based generators is connected to a DC urban distribution system, interfaced with a BDCR-FCL.

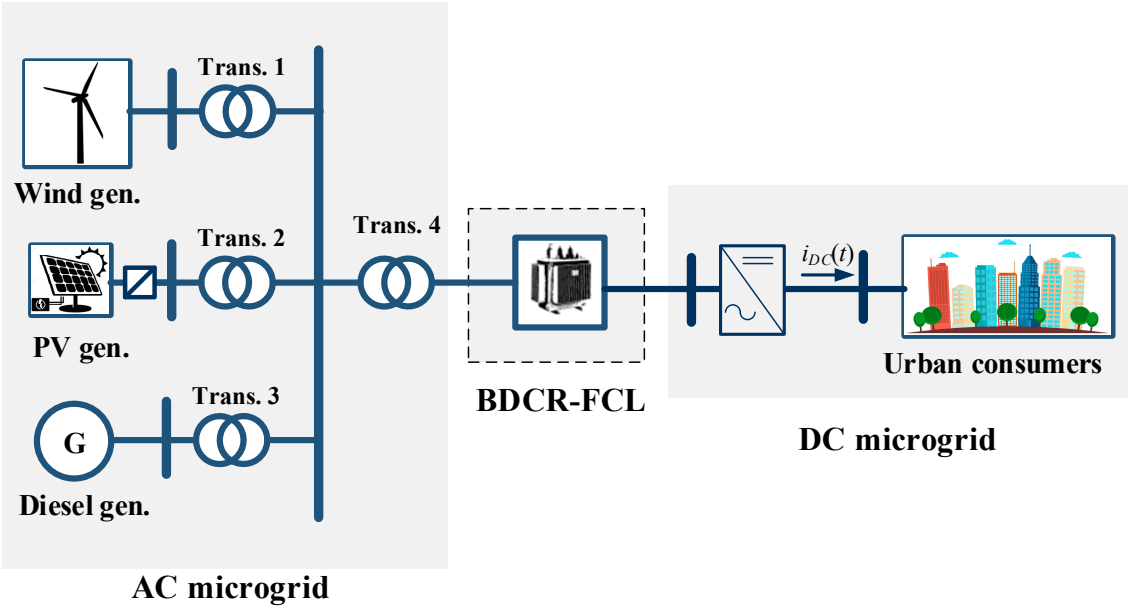

Figure 4. A BDCR-FCL interfaced with an AC/DC microgrid.

3. Analytical Study on Functionalities of BDCR-FCL

In this section, analytical studies have been carried out based on the three cases explained in the previous section. To such an aim, mathematical relationships have been derived and verified by the results obtained through simulation studies using PSCAD-EMTDC software for each of the described test cases. PSCAD/EMTDC is powerful software for time-domain simulation of electrical systems that solves differential equations of the

circuit based on Dommel's method [28]. This software has been chosen due to its high level of precision, which renders its results close to reality.

3.1. Analysis of an AC/DC Microgrid Interconnect without BDCR-SFCL (Case 1)

In an AC-to-DC microgrid interface, the power is transformed from one side to the other through a power electronic-based converter. Here, a quality assessment is conducted on the power flow and voltage harmonics caused by the nonlinear behavior of the converter and the DC side loads. In order to maintain the tractability of the analysis, the AC/DC converter is considered a simple bridge rectifier. The specifications of the considered test system are listed in Table 1.

Table 1. Specifications of the Case 1 test system.

Symbol	Quantity	Value
V_{ac}	AC microgrid Thevenin voltage	220 V_{RMS}
r	AC microgrid Thevenin resistance	0.1 Ω
R	DC system load	100 Ω
C	DC line shunt capacitor	1 mF

The duration of current flow in the shunt capacitor depends on the C value, the AC side equivalent resistance r, and the DC system load R. The test system demonstrated in Figure 1 is simulated in PSCAD-EMTDC, and the obtained waveforms have been represented in Figure 5. As the voltages of the AC microgrid and the DC system have been depicted in Figure 5a, their current waveforms are shown in Figure 5b.

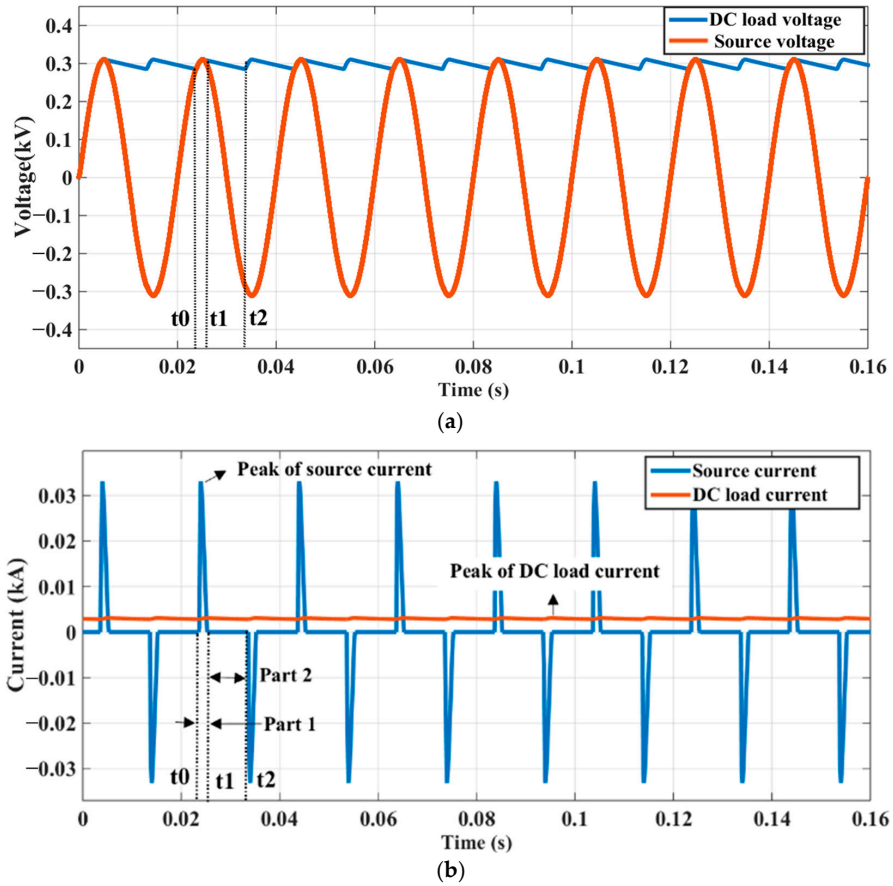

Figure 5. Results obtained from the simulation of the Case 1 test system: (**a**) AC microgrid and DC load voltages during the capacitor charging and discharging intervals; (**b**) AC microgrid current and DC load current during capacitance charging and discharging intervals.

As shown in Figure 5, the analysis of the test system can be carried out in two intervals, as explained below.

3.1.1. Operational Part 1: $t_0 \leq t \leq t_1$

In this interval, Kirchhoff's voltage law yields:

$$V_{ac}(t) - ri_L(t) - v_C(t) - v_R = 0 \tag{1}$$

where v_R is the converter voltage drop and v_C is the shunt capacitor's voltage, while V_{ac} and i_{ac} correspond to the voltage and the current of the AC microgrid. Considering that the rectifier is ideal, v_R would be equal to zero and thus:

$$v_C(t) = V_{ac}(t) - ri_{ac}(t);\ t_0 \leq t \leq t_1 \tag{2}$$

The AC microgrid voltage is assumed as a sinusoidal waveform with the peak value of V_m and frequency f, as:

$$V_{ac}(t) = V_m \sin(2\pi ft) \tag{3}$$

Therefore, the DC load current can be calculated by:

$$i_L(t) = \frac{v_C(t)}{R} \tag{4}$$

and the microgrid current is given by:

$$i_{ac}(t) = C\frac{dv_c(t)}{dt} + \frac{v_C(t)}{R} \tag{5}$$

3.1.2. Operational Part 2: $t_1 \leq t \leq t_2$

In this interval, the DC load voltage is the same as the capacitor and the DC line voltage. Therefore, the DC load current is equal to the capacitor discharge current. Therefore, the capacitor voltage is represented as:

$$v_c(t) = V_{ac}(t) - ri_{ac}(t) \tag{6}$$

and while in this operation mode, the AC microgrid delivers zero current to the DC system, thus $i_{ac}(t) = 0$. In this regard, the following yields:

$$C\frac{dv_c(t)}{dt} + \frac{v_C(t)}{R} = 0 \tag{7}$$

Accordingly, the DC load current will be equal to the capacitor discharge current and is therefore equal to an exponential decay at the RC time constant with the initial value of $v_c(t_1)/R$, calculated as:

$$i_L(t) = \frac{v_c(t_1)}{R} e^{\frac{-t}{RC}} \tag{8}$$

As demonstrated in Figure 6, the peak value of the AC microgrid current increases with the incorporation of the smoothing capacitor. From an energy balance perspective, the energy transmitted from the AC microgrid to the DC load must remain constant for every cycle; therefore, the area obtained from multiplying the AC microgrid current with the line voltage should remain constant as well. Considering the line voltage does not change, the larger the peak current is, the narrower its conducting time is. Therefore, using a larger shunt capacitor in the DC line causes severe di/dt in the AC microgrid current. Although higher values of capacitance may decrease the ripple in the DC load voltage, it increases the current harmonic generation in the AC microgrid.

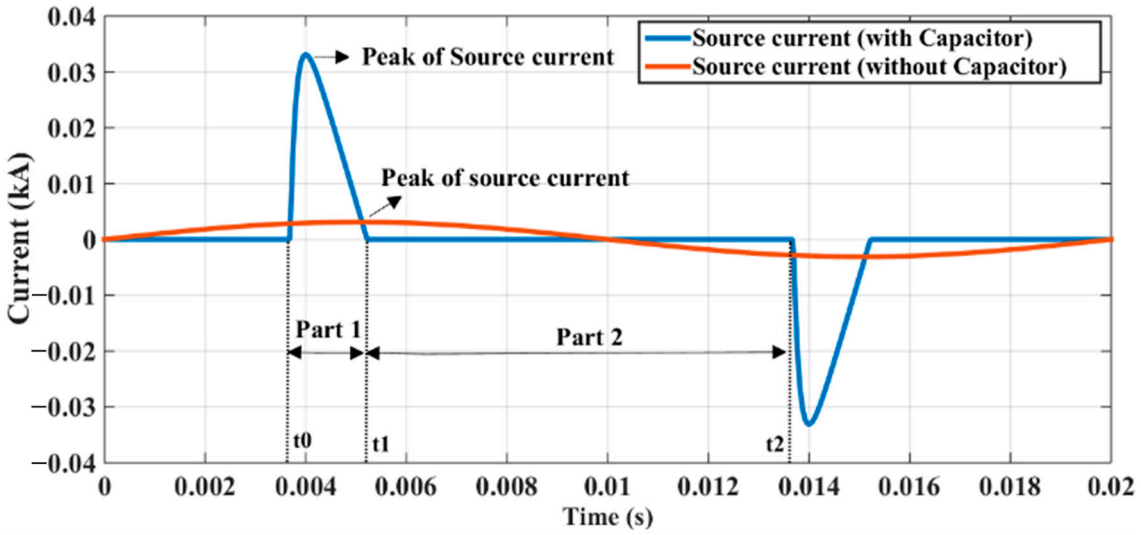

Figure 6. AC source current with and without shunt capacitor in Case 1.

3.2. Analysis of BDCR-FCL Effect in AC Microgrid Feeding an AC Load (Case 2)

In this case, the BDCR-FCL is connected in series to an AC load fed by the AC microgrid. During the steady-state condition, the BDCR-FCL current i_{DCR} has a negligible ripple, which depends on the BDCR-FCL parameter values. However, when a sudden change in the load value occurs, the current i_{DC} changes, as shown in Figure 7.

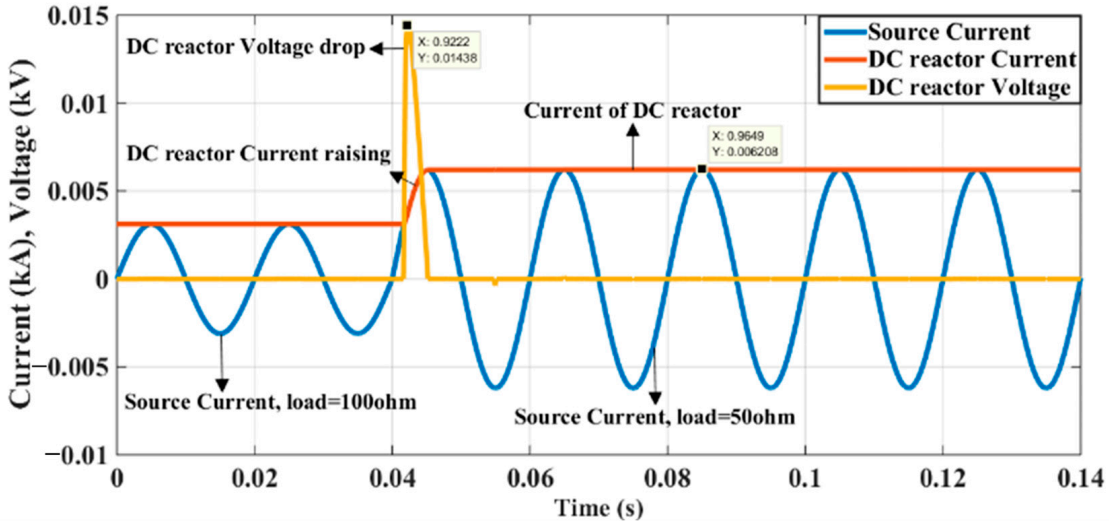

Figure 7. AC source current, BDCR-FCL current, and BDCR-FCL voltage drop in Case 2.

In these conditions, the current variation of the BDCR-FCL causes a voltage drop on the reactor, smoothing the load and source current variation as well. In order to demonstrate such an effect, in this simulation, the AC load is changed from 100 Ω to 50 Ω. Initially, the circuit contains only one load branch with a 100 Ω resistance. Subsequently, the load change is applied by activating a second 100 Ω branch in parallel, resulting in a total load of 50 Ω. Before the load variation, the BDCR-FCL can be considered bypassed, whereas upon the load change, its voltage increases, limiting the source current transients. Figure 7 shows the AC electrical source and BDCR-FCL currents before and after load variation. Specifications of the simulation case are provided in Table 2.

Table 2. Specifications of Case 2 test system.

Symbol	Quantity	Value
V_{ac}	AC microgrid Thevenin voltage	220 V_{RMS}
r	AC microgrid Thevenin resistance	0.1 Ω
R_1	System load branch 1	100 Ω
R_2	System load branch 2	100 Ω
L_d	BDCR-FCL inductance	100 mH
r_d	BDCR-FCL resistance	0.05 Ω
V_{FB}	Rectifier bridge voltage drop	0.7 V

3.3. Analysis of BDCR-FCL Effect on AC Microgrid Connected to DC Line (Case 3)

To analyze this case, the topology shown in Figure 3 is simulated in PSCAD-EMTDC software with the specifications tabulated in Table 3. The DC rectifier feeding the DC system acts as a nonlinear load to the AC microgrid. Figure 8a shows the obtained simulation results for the nonlinear DC load, BDCR-FCL, and AC microgrid current waveforms. The BDCR-FCL current is a DC with a negligible ripple, and the load current is a DC with a smaller value compared to the BDCR-FCL current. As shown in Figure 8a, the AC microgrid current has an AC nature and is contaminated with harmonic components. The source current with and without local BDCR-FCL is shown in Figure 8b. As characterized in the figures, by connecting the BDCR-FCL, the peak value of the AC microgrid current is decreased by 15 A, and the duration of each conduction cycle is increased by 1.6 ms as well. It is also important to note that using series BDCR-FCL improves the THD value of the source current for nonlinear loads, as shown in Figure 8c. The figure demonstrates the fundamental current component together with the 3rd, 5th, 9th, 11th, 13th, and 15th harmonic currents with and without the BDCR-FCL, clarifying that the amplitudes of low harmonics are decreased, while at the same time, the fundamental current component magnitude is increased.

Table 3. Specifications of Case 3 test system.

Symbol	Quantity	Value
V_{ac}	AC microgrid Thevenin voltage	220 V_{RMS}
r	AC microgrid Thevenin resistance	0.1 Ω
R	DC system load	100 Ω
L_d	BDCR-FCL inductance	100 mH
r_d	BDCR-FCL resistance	0.05 Ω
V_{FB}	Rectifier bridge voltage drop	0.7 V

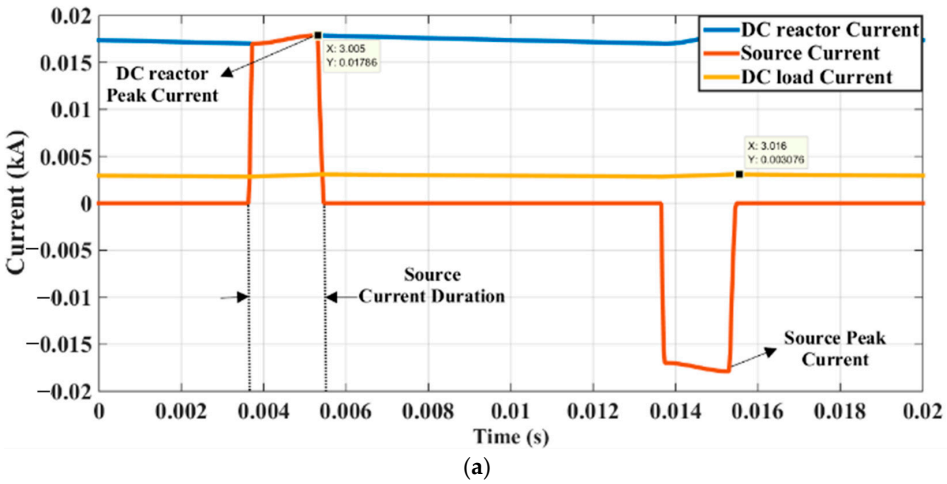

(**a**)

Figure 8. *Cont.*

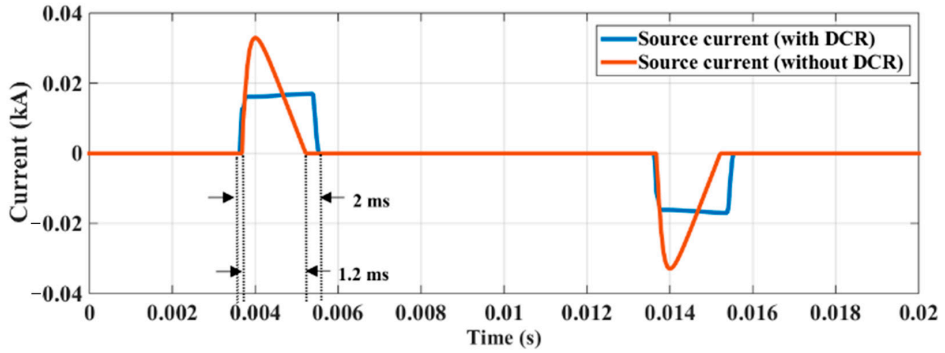

(**b**)

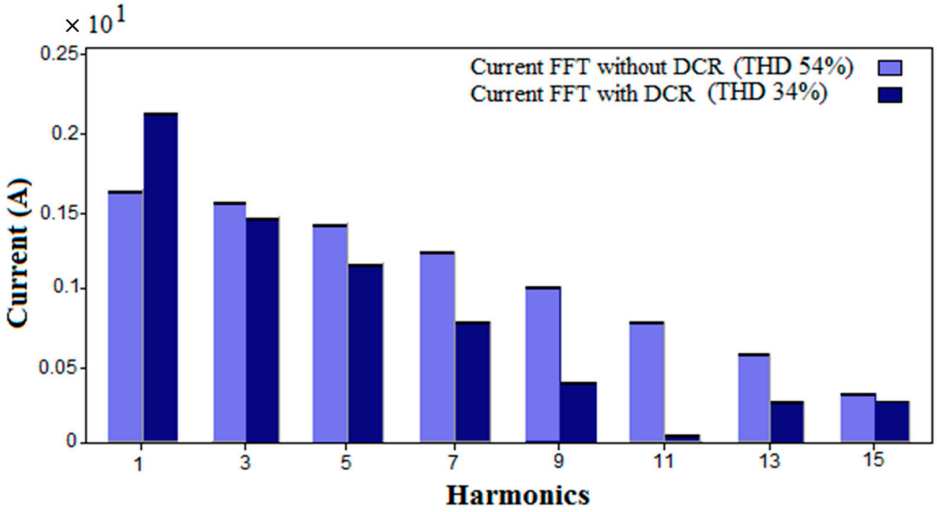

(**c**)

Figure 8. Results obtained from the simulation of the Case 3 test system. (**a**) DC load, BDCR-FCL, and AC source currents (**b**) AC source current with and without BDCR-FCL. (**c**) Harmonic spectrum of the AC source current referred to 50 Hz with and without BDCR-FCL.

The behavior of the BDCR-FCL in an AC microgrid can be analyzed based on the following equations:

$$i_{DC} = \text{Max}(i_{ac}(t)) \tag{9}$$

$$|i_{ac}(t)| = \frac{|V_{ac}(t)| - r_d i_{DC}(t)}{r + R} \tag{10}$$

$$v_{DCR}(t) = L_d \frac{di_{DC}(t)}{dt} + r_d i_{DC}(t) \tag{11}$$

Equations (9) and (10) describe the steady-state operation of the test system. In the steady state, due to the low resistance of the DC reactor, the current ripple is negligible. The dynamics of the BDCR-FCL are characterized in (11), with v_{DCR} denoting the voltage drop of BDCR-FCL. During the steady-state condition, while the BDCR-FCL current is almost a DC, Equation (11) can be rewritten as:

$$v_{DCR}(t) = r_d i_{DC}(t) \tag{12}$$

Equation (9) represents the initial current of the BDCR-FCL where it is charged to the peak value of the AC current. At this point, the voltage drop on the rectifier bridge diodes is almost zero. In the case of a load variation, the BDCR-FCL current increases, raising the voltage drop of the BDCR-FCL in accordance with Equation (11). Consequently, the voltage of the load is reduced, and thus the rate of rise of current in the AC microgrid is decreased.

The BDCR-FCL can also introduce power factor correction capabilities. Power factor is affected by two issues: current displacement and waveform distortions. The former is

caused by the displacement between the source current and voltage by an angle φ, whereas the latter is caused by the presence of harmonic components. The overall power factor, considered to evaluate the performance of BDCR-FCL, is calculated as follows [29]:

$$\mathrm{PF} = PF_{CD} \times PF_{DPF} \tag{13}$$

where PF_{CD} is the current displacement PF and PF_{DPF} is the distortion PF, given by [29]:

$$PF_{CD} = \cos\varphi \tag{14}$$

$$PF_{DPF} = \frac{1}{\sqrt{1+THD^2}} = \frac{I_1}{\sqrt{{I_1}^2 + \sum_{n=2}^{k} {I_n}^2}} \tag{15}$$

where I_1 is the fundamental component of the current and n is the harmonic order. As shown in Figure 8c, the total distortion of the AC microgrid current is enhanced by 20%. According to (15), this corresponds to the improvement of the PF_{DPF} from 0.88 to around 0.947. Therefore, the total PF will accordingly improve by using series BDCR-FCL. It is important to note that the PF and amount of harmonic pollution studied here have been considered extreme conditions to demonstrate the alleviative capabilities of the BDCR-FCL in improving even the most extreme THDs and PFs. Supported by obtained results, the effect of BDCR-FCL on reducing the harmonics and improving the PF is validated.

4. Experimental Analysis

The experimental tests have been carried out on a scaled down prototype laboratory setup, including a BDCR-FCL, which is utilized to confirm the analytical studies. The laboratory setup is in the form of the topology in Figure 3 (Case 3). Tests have been conducted to demonstrate the multifaceted functionalities of the BDCR-FCL to improve PF, THD, and rate of rise of current, and to smooth the load variation alongside providing fault current limitation capabilities. Setup parameters are listed in Table 4, and the prototype configuration is shown in Figure 9. It is to be noted that the setup is fed by an autotransformer, and the DC reactor is composed of an E-I magnetic core and 50 turns of wire. This DC reactor, under normal condition, enforces a constant current of 2 A. The signals are measured by means of a digital oscilloscope and are further imported into a computer for post-processing studies.

Table 4. Specifications of experimental test setup.

Symbol	Quantity	Value
V_{ac}	Source voltage	220 V_{RMS}
R	DC load	100 Ω
L_{d}	BDCR-FCL inductance	100 mH
r_{d}	BDCR-FCL resistance	0.1 Ω
C	DC line shunt capacitor	1 mF
D	Rectifier bridge diode	1N5819
V_{FB}	Rectifier bridge voltage drop	0.7 V

The results obtained from the tests conducted on the experimental setup are demonstrated in Figure 10. The source voltage, representing the AC microgrid, is illustrated in Figure 10a, where the visible intrinsic harmonic distortions are due to the grid line voltage. This voltage feeds the DC system, which includes the rectifier, smoothing capacitor, and DC load with and without the series BDCR-FCL. Figure 10b,c show the source current with and without BDCR-FCL, respectively. The metrics considered to evaluate the effect of BDCR-FCL are the current peak value, the time duration of current conduction in a cycle, and the rate of rise of the current. As seen in Figure 10b, the current peak value is 1.7 A, and the duration of current conduction is 3.5 ms, resulting in the rate of rise of current equal to 486 A/s, similar to the results depicted in Figures 6 and 8a. As shown in Figure 10c, the

quality of the source current waveform is improved by using BDCR-FCL. In this figure, the current peak value is 0.6 A, and the current conduction duration in one half-cycle is 6 ms, thus limiting its rate of rise of current to around 100 A/s, which agrees with the results in Figure 8a,b. In addition, as illustrated in Figure 10d, the BDCR-FCL current matches the absolute value of the source current during the capacitor charging intervals.

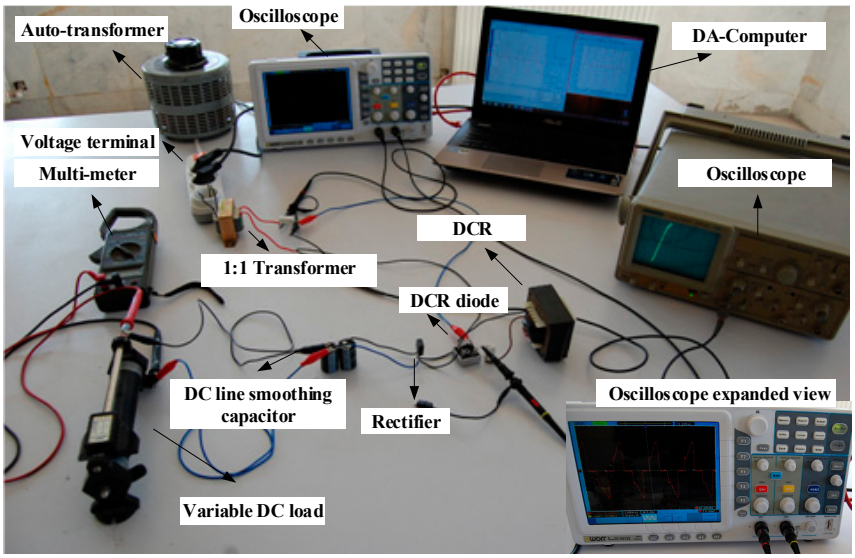

Figure 9. Scaled down laboratory test setup.

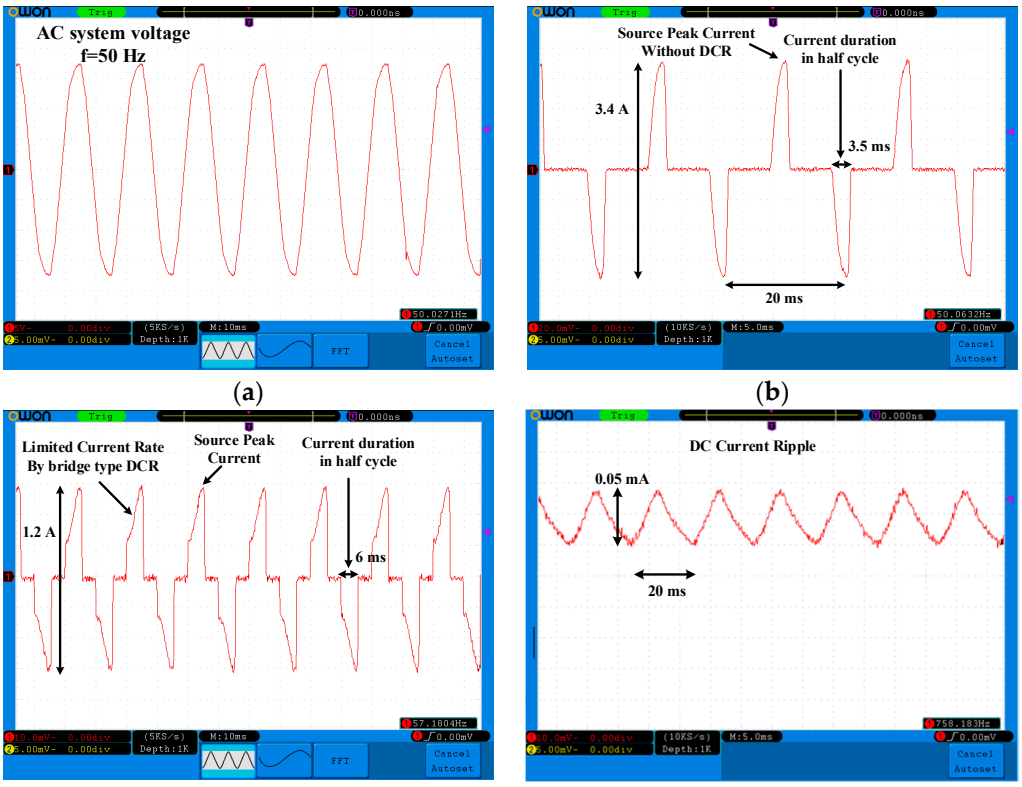

Figure 10. Experimental test setup results, red curved demonstrating waveforms for: (**a**) Source voltage (transformer output). (**b**) Source current without BDCR-FCL. (**c**) Source current with BDCR-FCL. (**d**) BDCR-FCL current.

Fourier analyses of the source current harmonic spectrum with and without BDCR-FCL are presented in Figures 11a and 11b, respectively. The experimental results demonstrate that THD is improved by 18%, which verifies the harmonic restraining effect of BDCR-FCL. Moreover, according to Equation (15), the THD enhancement shown in Figure 11 results in the improvement of distortion PF from 0.86 to 0.93, validating the effect of BDCR-FCL in improving the PF.

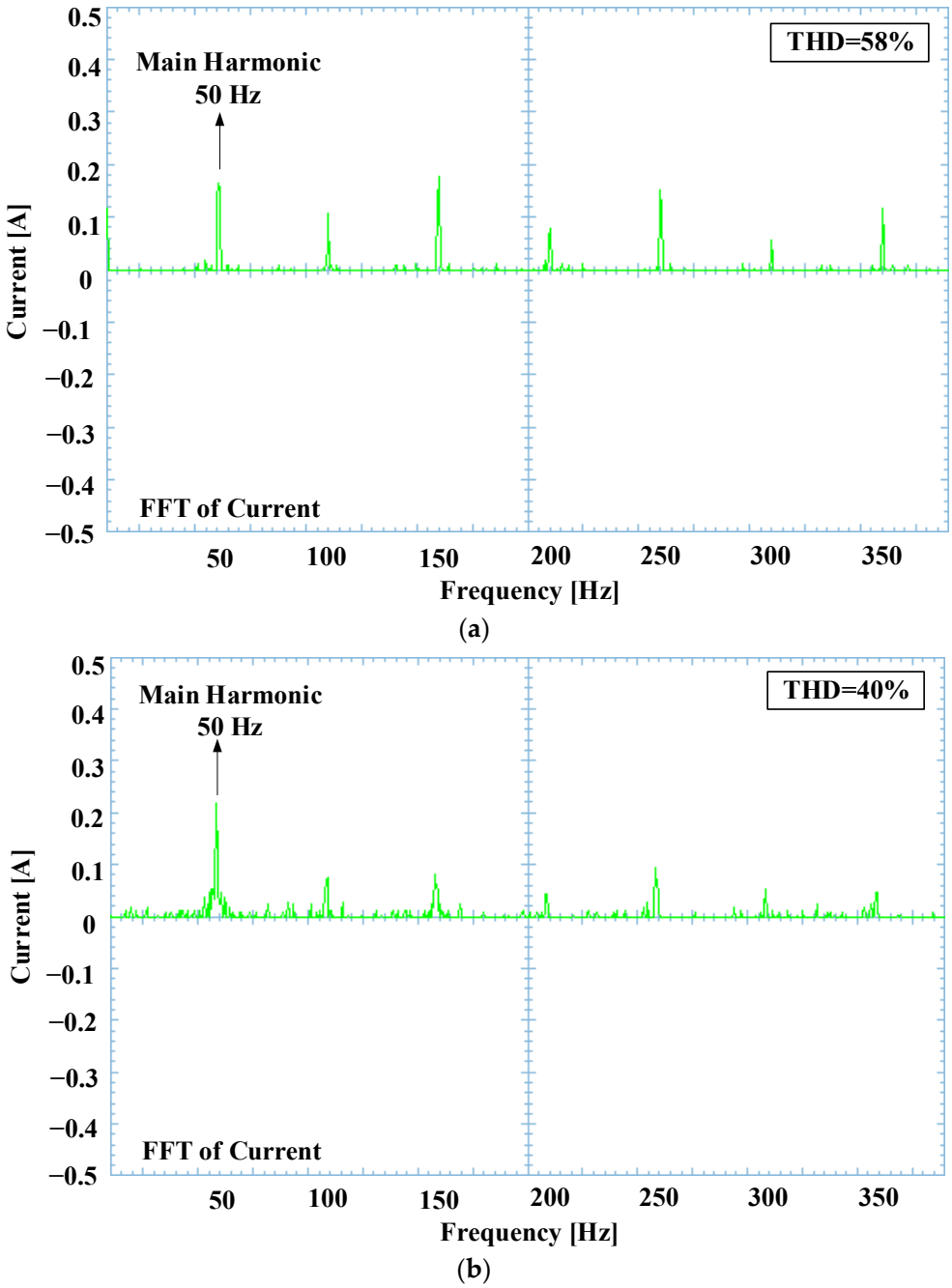

Figure 11. Harmonic spectrum analysis of AC source current. (**a**) Without the incorporation of BDCR-FCL. (**b**) With the incorporation of BDCR-FCL.

5. Discussion

According to the simulation analyses and laboratory experiments, it was demonstrated that BDCR-FCLs can be far more effective devices for connecting AC microgrids to DC systems because by employing BDCR-FCLs, alongside the limitation of fault current, soft

load starting is achieved by decreasing the rate of rise of current, the peak current of nonlinear loads is alleviated, the THD of source current is improved, and consequently an overall improvement in power quality is attained, while no external control is involved in its operation either. In this regard, the THD was shown to be improved by 20% and 18% in the simulation and the experimental cases, respectively, and the PF was shown to be improved through enhancement of distortion PF from 0.88 to 0.947 in the simulation case and from 0.86 to 0.93 in the experimental case.

Unlike other FCL technologies, which are only present in the current flow path under the faulty condition, the BDCR-FCL is not bypassed in the non-faulty condition. Therefore, BDCR-FCLs can provide such additional functionalities as discussed by disagreeing variations even under non-faulty conditions. In this regard, the functionalities of the BDCR-FCL can be compared with the most prominent FCL technologies, i.e., the reactor type [5] and the superconductor type [7] FCLs, as presented in Table 5.

Table 5. Comparison of FCL technologies in terms of functionalities.

Technology	Fault Current Limiting	Waveform Smoothing	PF Enhancement	THD Reduction
Reactor type [5]	Yes	No	No	No
Superconductor type [7]	Yes	No	No	No
BDCR	Yes	Yes	Yes	Yes

It is worth mentioning that although the experimental tests were conducted for a scaled down laboratory test setup, similar outcomes, i.e., THD reduction, PF enhancement, and waveform correction capabilities, can be expected on a real scale. However, it is important to bear in mind that at the grid scale, specialized power electronic components would have to be employed, and the circuit design would require special care, complying with the insulation coordination necessities, particularly to handle the high voltage levels. The advantages of the BDCR-FCLs are listed in Table 6.

Table 6. Summary of the BDCR-FCL advantages.

Issue	BDCR-FCL Effect
Nonlinear load peak current	Limits the nonlinear load peak
Nonlinear load conduction duration	Increases nonlinear load conduction duration
THD	Reduces the current THD
PF	Improves the PF
Load current variations	Smooths the load current variations
Rate of rise of current	Reduced rate of rise of current
Reactive power loss	No notable reactive power as a DC inductor

6. Conclusions

In this paper, a comprehensive analysis of a BDCR-FCL was carried out. The investigations of this paper were performed through simulated case studies and experimental tests, validating the superior functionalities of BDCR-FCLs. This study shows that BDCR-FCLs can present additional capabilities, extending beyond its primary role as a fault current-limiting device. This device can provide waveform distortion improvement, reducing the current THD and correcting the PF in power networks. It was also proved that BDCR-FCLs enhance the current conduction duration, reduce the rate of rise of current, and thus limit the peak current of nonlinear loads and smooth the load variations. Moreover, as BDCR-FCLs are essentially series DC inductors, they do not consume reactive power during steady-state conditions. Overall, the BDCR-FCL presents promising capabilities in enhancing power quality alongside limiting fault currents. Its multifunctional characteristics make it a viable option for integration into microgrid applications, contributing to the resilience and sustainability of the power grid.

Author Contributions: Conceptualization, B.B., A.M., S.M. and M.S.; investigation, A.M., S.M. and M.S.; methodology, B.B., A.M., S.M. and M.S.; writing—original draft preparation, B.B., A.M., S.M. and M.S.; writing—review and editing, B.B. and M.H.; supervision, B.B. and M.H.; interpretation of data, B.B., A.M., S.M. and M.S.; accuracy and integrity assurance, B.B. and M.H.; validation, B.B.; final approval, M.H. All authors have read and agreed to the published version of the manuscript.

Funding: This research received no external funding.

Data Availability Statement: Data will be made available on request.

Conflicts of Interest: The authors declare no conflict of interest.

References

1. Safaei, A.; Zolfaghari, M.; Gilvanejad, M.; Gharehpetian, G.B. A survey on fault current limiters: Development and technical aspects. *Int. J. Electr. Power Energy Syst.* **2020**, *118*, 105729. [CrossRef]
2. Behdani, B.; Shariatinasab, R.; Afrasiabi, M.; Aghaei, J. Analysis of Power Transformer Inrush Current in the Presence of Quasi-Direct Currents. In Proceedings of the 2022 IEEE International Conference on Environment and Electrical Engineering and 2022 IEEE Industrial and Commercial Power Systems Europe (EEEIC/I & CPS Europe), Prague, Czech Republic, 28 June–1 July 2022; pp. 1–6. [CrossRef]
3. El-Ela, A.A.A.; El-Sehiemy, R.A.; Shaheen, A.M.; Ellien, A.R. Review on active distribution networks with fault current limiters and renewable energy resources. *Energies* **2022**, *15*, 7648. [CrossRef]
4. Pulido, E.; Morán, L.; Villarroel, F.; Silva, J. Active reduction of short-circuit current in power distribution systems. *Energies* **2020**, *13*, 334. [CrossRef]
5. Ibrahim, R.A.; Zakzouk, N.E. Bi-functional non-superconducting saturated-core inductor for single-stage grid-tied PV systems: Filter and fault current limiter. *Energies* **2023**, *16*, 4206. [CrossRef]
6. Kartijkolaie, H.S.; Hsia, K.-H.; Mobayen, S.; Firouzi, M.; Shafiee, M. Controllable-dual bridge fault current limiter for interconnection micro-grids. *Energies* **2021**, *14*, 1026. [CrossRef]
7. Afrasiabi, S.; Behdani, B.; Afrasiabi, M.; Mohammadi, M.; Asheralieva, A.; Gheisari, M. Differential Protection of Power Transformers based on RSLVQ-Gradient Approach Considering SFCL. In Proceedings of the 2021 IEEE Madrid PowerTech, Madrid, Spain, 28 June–2 July 2021; pp. 1–6. [CrossRef]
8. Heidary, A.; Yazdani-Asrami, M.; Hesami, M.; Sood, V. The TRV Improvement of Fast Circuit Breakers Using Solid-State Series Superconducting Reactor. *IEEE Trans. Power Deliv.* **2023**, *38*, 1259–1266. [CrossRef]
9. You, H.; Jin, J. Characteristic analysis of a fully controlled bridge type superconducting fault current limiter. *IEEE Trans. Appl. Supercond.* **2016**, *26*, 5603706. [CrossRef]
10. Heidary, A.; Popov, M.; Moghim, A.; Niasar, M.G.; Lekić, A. The Principles of Controlled DC-Reactor Fault Current Limiter for Battery Energy Storage Protection. *IEEE Trans. Ind. Electron.* **2024**, *71*, 1525–1534. [CrossRef]
11. Heidary, A.; Radmanesh, H.; Rouzbehi, K.; Pou, J. A DC-Reactor-Based Solid-State Fault Current Limiter for HVdc Applications. *IEEE Trans. Power Deliv.* **2019**, *34*, 720–728. [CrossRef]
12. Heidary, A.; Radmanesh, H.; Moghim, A.; Ghorbanyan, K.; Rouzbehi, K.; MGRodrigues, E.; Pouresmaeil, E. A multi-inductor H bridge fault current limiter. *Electronics* **2019**, *8*, 795. [CrossRef]
13. Heidary, A.; Radmanesh, H.; Bakhshi, A.; Samandarpour, S.; Rouzbehi, K.; Shariati, N. Compound ferroresonance overvoltage and fault current limiter for power system protection. *IET Energy Syst. Integr.* **2020**, *2*, 325–330. [CrossRef]
14. *IEEE Std 519-2022 (Revision of IEEE Std 519-2014)*; IEEE Standard for Harmonic Control in Electric Power Systems. IEEE: Piscataway, NJ, USA, 2022; pp. 1–31. [CrossRef]
15. *IEEE Std 1547-2003*; IEEE Standard for Interconnecting Distributed Resources with Electric Power Systems. IEEE: Piscataway, NJ, USA, 2003; pp. 1–28. [CrossRef]
16. Heidary, A.; Radmanesh, H.; Rouzbehi, K.; Mehrizi-Sani, A.; Gharehpetian, G.B. Inductive fault current limiters: A review. *Electr. Power Syst. Res.* **2020**, *187*, 106499. [CrossRef]
17. Heidary, A.; Rouzbehi, K.; Mehrizi-Sani, A.; Sood, V.K. A Self-Activated Fault Current Limiter for Distribution Network Protection. *IEEE J. Emerg. Sel. Top. Power Electron.* **2022**, *10*, 4626–4633. [CrossRef]
18. Carbone, R.; Scappatura, A. A high efficiency passive power factor corrector for single-phase bridge diode rectifiers. In Proceedings of the 2004 IEEE 35th Annual Power Electronics Specialists Conference (IEEE Cat. No.04CH37551), Aachen, Germany, 20–25 June 2004; Volume 2, pp. 1627–1630. [CrossRef]
19. Sainz, L.; Pedra, J.; Mesas, J.J. Single-phase full-wave rectifier study with experimental measurements. *Electr. Power Syst. Res.* **2007**, *77*, 339–351. [CrossRef]
20. Beres, R.N.; Wang, X.; Liserre, M.; Blaabjerg, F.; Bak, C.L. A Review of Passive Power Filters for Three-Phase Grid-Connected Voltage-Source Converters. *IEEE J. Emerg. Sel. Top. Power Electron.* **2016**, *4*, 54–69. [CrossRef]
21. Rockhill, A.A.; Liserre, M.; Teodorescu, R.; Rodriguez, P. Grid-Filter Design for a Multimegawatt Medium-Voltage Voltage-Source Inverter. *IEEE Trans. Ind. Electron.* **2011**, *58*, 1205–1217. [CrossRef]

22. Beres, R.N.; Wang, X.; Blaabjerg, F.; Bak, C.L.; Liserre, M. Comparative analysis of the selective resonant LCL and LCL plus trap filters. In Proceedings of the 2014 International Conference on Optimization of Electrical and Electronic Equipment (OPTIM), Bran, Romania, 22–24 May 2014; pp. 740–747. [CrossRef]
23. Beres, R.N.; Wang, X.; Blaabjerg, F.; Liserre, M.; Bak, C.L. Optimal Design of High-Order Passive-Damped Filters for Grid-Connected Applications. *IEEE Trans. Power Electron.* **2016**, *31*, 2083–2098. [CrossRef]
24. Xie, X.; Huang, Z.; Fan, X.; Tang, T. Adaptive single-phase auto-reclosing scheme based on the moving average filter-quadrature signal generator for transmission lines with shunt reactors. *Electr. Power Syst. Res.* **2023**, *223*, 109545. [CrossRef]
25. Muhlethaler, J.; Schweizer, M.; Blattmann, R.; Kolar, J.W.; Ecklebe, A. Optimal Design of LCL Harmonic Filters for Three-Phase PFC Rectifiers. *IEEE Trans. Power Electron.* **2013**, *28*, 3114–3125. [CrossRef]
26. Jennings, G.; de Villiers, L. Transient Stability improvement using series reactors: A case study. In Proceedings of the 2015 IEEE Electrical Power and Energy Conference (EPEC), London, ON, Canada, 26–28 October 2015; pp. 296–302. [CrossRef]
27. Meral, M.E.; Çelik, D. Mitigation of DC-link voltage oscillations to reduce size of DC-side capacitor and improve lifetime of power converter. *Electr. Power Syst. Res.* **2021**, *194*, 107048. [CrossRef]
28. Dommel, H.W. *EMTP Theory Book*; Microtran Power System Analysis Corporation: Vancouver, BC, Canada, 1992.
29. Das, J.C. *Power System Harmonics and Passive Filter Designs*; John Wiley & Sons: Nashville, TN, USA, 2015.